Surface-Based Lithium Ion Sensor: An Electrode Derivatized with a Self-Assembled Monolayer

ARTICLE *in* ANALYTICAL CHEMISTRY · NOVEMBER 2006

Impact Factor: 5.64 · DOI: 10.1021/ac0603429 · Source: PubMed

4 AUTHORS, INCLUDING:

Nantanit Wanichacheva
Silpakorn University
20 PUBLICATIONS **177** CITATIONS

SEE PROFILE

Christopher R Lambert
Worcester Polytechnic Institute
67 PUBLICATIONS **1,501** CITATIONS

SEE PROFILE

Surface-Based Lithium Ion Sensor: An Electrode Derivatized with a Self-Assembled Monolayer

Nantanit Wanichacheva, Ernesto R. Soto, Christopher R. Lambert,* and W. Grant McGimpsey*

Department of Chemistry and Biochemistry, Worcester Polytechnic Institute, 100 Institute Road, Worcester, Massachusetts 01609

Self-assembled monolayers (SAMs) of 21-(16-mercaptohexadecan-1-oyl)-4,7,13,16-tetraoxa-1,10,21-triazabicyclo-[8.8.5]tricosane-19,23-dione were prepared on gold. Characterization of the SAMs was carried out by sessile drop contact angle, ellipsometry, grazing angle FT-IR spectroscopy, and electrochemical techniques. The cation recognition properties of the SAM were studied by cyclic voltammetry and impedance spectroscopy. The films show moderate selectivity for detection of Li^+ ions in solution over K^+ and Na^+, with selectivity values calculated to be $\log K_{Li^+,Na^+} \sim -1.30$ and $\log K_{Li^+,K^+} \sim -0.92$. To the best of our knowledge, this is the first demonstration of a lithium sensor fabricated using self-assembled monolayer technology.

Modification of gold surfaces with self-assembled monolayers (SAMs) of organic compounds has received considerable interest due to the potential application of such systems in the fields of microelectronics, friction control, photovoltaic devices, and sensors. The use of SAMs in sensor technology has typically used electrochemical techniques to transduce the binding of the analyte. For example, Deng et al.[1] prepared multilayers of thionine covalently tethered to an enzyme, horseradish peroxidase, for the preparation of an enzyme biosensor transduced by electron transfer. Cyclic voltammetry (CV) and impedance spectroscopy techniques allows the detection of an analyte binding to SAMs by measuring changes in conductivity or capacitance.[2−4] Reinhoudt and co-workers[5−8] have prepared SAMs of alkanethiols bearing crown ethers that can complex nonelectrochemically active ions, such as Na^+ and K^+, or metallosalophenes that complex transition metal ions (e.g. Ni^{2+}, $Cu^{2+}$and Co^{2+}) and have studied the binding process with CV and impedance techniques. The ion recognition properties of other molecules on gold, such as helical peptides linked to a crown ether,[9] crown ethers bonded to tetrathiafulvalene disulfides,[10,11] and alkanethiols modified with nitrilotriacetic acid have also been studied.[4]

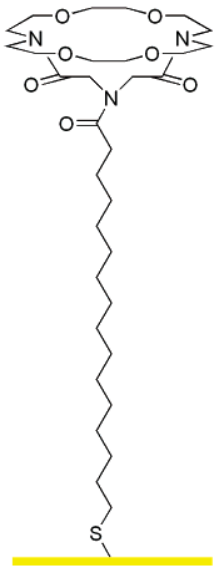

Figure 1. Structure of the Li^+ sensor on a gold surface.

We have previously reported the design, synthesis, and testing of highly selective new sensors for blood analytes. These sensors include an ammonium ionophore based on a cyclic depsipeptide structure,[12] a potassium fluoroionophore consisting of a 9-anthryl-substituted azacrown ether covalently linked to a 1,3-alternate calyx[4]arene,[13] a lithium fluoroionophore based on a *N*-(9-methylanthracene) moiety linked to a butylcalix[4]arene-azacrown,[14] and a sodium ion sensor based on a covalently linked aminorhodamine calyx[4]arene.[15]

* Corresponding author. Phone: 508-831-5486. Fax: 508-831-5933. E-mail: wgm@wpi.edu.

(1) Ruan, C.; Yang, F.; Lei, C.; Deng, J. *Anal. Chem.* **1998**, *70*, 1721−1725.
(2) Gafni, Y.; Weizman, H.; Libman, J.; Shanzer, A.; Rubinstein, I. *Chem.—Eur. J.* **1996**, *2*, 759−766.
(3) Stora, T.; Hovius, R.; Dienes, Z.; Pachoud, M.; Vogel, H. *Langmuir* **1997**, *13*, 5211−5214.
(4) Henke, C.; Steinem, C.; Janshoff, A.; Steffan, G.; Luftmann, H.; Sieber, M.; Galla, H. J. *Anal. Chem.* **1996**, *68*, 3158−3165.
(5) Beulen, M. W. J.; Van Veggel, F. C. J. M.; Reinhoudt, D. N. *Isr. J. Chem.* **2000**, *40*, 73−80.
(6) Flink, S.; Boukamp, B. A.; van den Berg, A.; van Veggel, F. C. J. M.; Reinhoudt, D. N. *J. Am. Chem. Soc.* **1998**, *120*, 4652−4657.
(7) Flink, S.; van Veggel, F. C. J. M.; Reinhoudt, D. N. *J. Phys. Chem. B.* **1999**, *103*, 6515−6520.
(8) Flink, S.; van Veggel, F. C. J. M.; Reinhoudt, D. N. *Adv. Mater.* **2000**, *12*, 1315−1328.
(9) Miura, Y.; Kimura, S.; Kobayashi, S.; Imanishi, Y.; Umemura, J. *Biopolymers* **2001**, *55*, 391−398.
(10) Liu, H.; Liu, S.; Echegoyen, L. *Chem. Commun.* **1999**, 1493−1494.
(11) Liu, S.-G.; Liu, H.; Bandyopadhyay, K.; Gao, Z.; Echegoyen, L. *J. Org. Chem.* **2000**, *65*, 3292−3298.
(12) Benco, J. S.; Nienaber, H. A.; McGimpsey, W. G. *Anal. Chem.* **2003**, *75*, 152−156.
(13) Benco, J. S.; Nienaber, H. A.; Dennen, K.; McGimpsey, W. G. *J. Photochem. Photobiol., A* **2002**, *152*, 33−40.
(14) Benco, J. S.; Nienaber, H. A.; McGimpsey, W. G. *J. Photochem. Photobiol., A* **2004**, *162*, 289−296.

This paper reports the results for a Li^+ sensor fabricated from a self-assembled monolayer on gold. The SAM comprises a single molecular layer of a bicyclic structure shown in Figure 1. Related work on the ionophore moiety linked to a fluorophore showed high selectivity for Li^+ against the interfering ions NH_4^+, Na^+, and K^+ in solution.[16] Monitoring of Li^+ in blood is necessary for patients who suffer from manic depressive and hyperthyroidism illnesses and who are treated with lithium salts.

The compound shown in Figure 1 consists of a 4,7,13,16-tetraoxa-1,10,21-triazabicyclo[8.8.5]tricosane-19,23-dione attached to a hexadecanethiol chain. This compound was designed following an approach similar to the one that was used for our previously reported ionophores and fluoroionophores. Molecular modeling of the bicyclic structure showed that it provides a semirigid framework and size fit for a lithium ion. A hexadecanethiol molecule was used to form a relatively ordered self-assembled monolayer on gold with the bicyclic moieties exposed on the surface. The lithium ion binding ability of the surface-bound sensor was monitored by cyclic voltammetry and impedance spectroscopy according to procedures previously described by Reinhoudt and others.[5−11,17]

Materials. All reagents and solvents for synthesis were purchased from Aldrich and were used as received unless otherwise noted. *N*-Fmoc-iminodiacetic acid was purchased from Fluka Chemical Corporation (Milwaukee, WI). Poly(vinyl chloride) high molecular weight (PVC) and dioctyl phthalate (DOP) were purchased from Fluka (Bush, Switzerland). Electrolyte solutions were freshly prepared using high-purity Millipore deionized water (18 MΩ.cm).

General Methods. NMR spectra were obtained in an Avance Bruker spectrometer at 400 MHz for proton and 100 MHz for ^{13}C. All NMR spectra were obtained in $CDCl_3$ solutions unless otherwise indicated. Mass spectra were measured by SynPep Corporation (Dublin, CA). Ionization was performed using electrospray using acetonitrile as the carrier solvent and nitrogen as a curtain gas.

Synthesis. The synthesis of the compound used for the preparation of the SAM shown in Figure 1 was performed according to the synthetic steps outlined in Scheme 1.

9*H*-9-Fluorenylmethyl-19,23-dioxo-4,7,13,16-tetraoxa-1,10,21-triazabicyclo[8.8.5]tricosane-21-carboxylate. In a round-bottom flask, 1.78 g (5 mmol) of *N*-Fmoc-iminodiacetic acid was dissolved in 15 mL (206 mmol) of thionyl chloride, and the solution was heated at reflux for 30 min. The excess of thionyl chloride was then removed under reduced pressure at 40 °C, and the residue was dissolved in 250 mL of dichloromethane. A sample of 1.31 g (4.9 mmol) of diaza-18-crown-6 and 2.6 mL (14.4 mmol) of diisopropylethylenediamine (DIPEA) was added to the dichloromethane solution. The mixture was stirred for 7 h at room temperature. DIPEA and the solvent were removed by evaporation of the mixture under reduced pressure, and the residue was redissolved in 100 mL of dichloromethane. The solution was washed three times with 100 mL of 2 N HCl and once with 100 mL of water and, finally, dried over anhydrous $MgSO_4$. The solvent was finally removed under reduced pressure to yield a white solid residue, which was purified by flash column chromatography (Biotage Flash 40 column 15 cm × 7 cm, CH_2Cl_2/CH_3OH 15:1). mp = 181−182 °C. Yield: 2.0 g (70%). R_f = 0.5 (CH_2Cl_2/CH_3OH 15:1). ^1H NMR (400 MHz, $CDCl_3$): δ 2.71−2.73 (m, 2H), 2.98−3.00 (m, 2H), 3.54−3.83 (m, 16H), 3.90−3.94 (m, 2H), 4.03−4.07- (d, J = 16.7 Hz, 1H), 4.11−4.15 (d, J = 16.7 Hz, 1H), 4.25−4.32 (m, 2H), 4.40−4.45 (m, 2H), 4.51 (dd, J = 6.1, 3.8 Hz, 1H), 4.58 (d, J = 16.7 Hz, 1H), 4.80 (d, J = 16.7 Hz, 1H), 7.22−7.40 (m, 4H), 7.60−7.64 (m, 2H), 7.73 (d, J = 7.6 Hz, 2H). ^{13}C NMR (100 MHz, $CDCl_3$): δ 42.3 (CH), 42.7 (CH_2), 42.8 (CH_2), 44.2 (CH_2), 44.4 (CH_2), 45.4 (CH_2), 45.5 (CH_2), 62.5 (CH_2), 62.7 (CH_2), 63.2 (CH_2), 65.5 (CH_2), 65.6 (CH_2), 66.1 (CH_2), 66.1 (CH_2), 66.7 (CH_2), 66.9 (CH_2), 114.9 (CH), 115.0 (CH), 120.4 (CH), 120.7 (CH), 122.2 (CH), 122.3 (CH), 122.6 (CH), 122.8 (CH), 123.0 (CH), 136.4 (CH), 136.4 (CH), 139.2 (CH), 139.6 (CH), 152.4 (C═O), 163.9 (C═O), 164.2 (C═O).

4,7,13,16-Tetraoxa-1,10,21-triazabicyclo[8.8.5]tricosane-19,23-dione. In a round-bottom flask, 0.49 g (0.84 mmol) of 9*H*-9-fluorenylmethyl-19,23-dioxo-4,7,13,16-tetraoxa-1,10,21-triazabicyclo-[8.8.5]tricosane-21-carboxylate was dissolved in 20 mL of 20% piperidine in CH_2Cl_2, and the solution was stirred for 30 min. The solvent was removed under reduced pressure at 40 °C to yield a light yellow gum. The product was purified by flash chromatography (Biotage Flash 40 column 15 cm × 7 cm, CH_3OH/Et_3N 25:1) to yield 0.28 g of a white solid. mp = 279−280 °C. Yield 93%. R_f = 0.4 (25:1 MeOH/Et_3N). ^1H NMR (400 MHz, $CDCl_3$): δ 2.68−2.74 (m, 2H), 2.90−2.96 (m, 2H), 3.48−3.70 (m, 18H), 3.77−3.85 (m, 2H), 3.89−3.94 (m, 2H), 4.33−4.37 (m, 2H). ^{13}C NMR (100 MHz, $CDCl_3$): δ 48.5 ($2CH_2$), 50.0 ($2CH_2$), 50.5 ($2CH_2$), 68.1 ($2CH_2$), 70.7 ($2CH_2$), 71.0 ($2CH_2$), 72.7 ($2CH_2$), 171.8 (2C═O).

21-(16-Bromohexadecanoyl)-4,7,13,16-tetraoxa-1,10,-21-triazabicyclo[8.8.5]tricosane-19,23-dione. In a round-bottom flask, 0.99 g (3 mmol) of 16-bromohexadecanoic acid was dissolved in 15 mL (15 mmol) of thionyl chloride. The solution was heated at reflux for 30 min. Thionyl chloride was removed under reduced pressure at 40 °C. The residue was dissolved in 30 mL of dichloromethane. To this solution, 1.11 g (3.1 mmol) of 4,7,13,16-tetraoxa-1,10,21-triazabicyclo[8.8.5]tricosane-19,23-dione and 1.4 mL (7.7 mmol) of DIPEA were added. The mixture was stirred at room temperature for 1 day. DIPEA and the solvent were removed from the solution by evaporation of the solvent mixture under reduced pressure, and the residue was redissolved in 100 mL of dichloromethane. The solution was washed three times with 100 mL of 2 N HCl and once with 100 mL of water and, finally, dried over anhydrous $MgSO_4$. The solvent was removed under reduced pressure, and the product was finally purified by column chromatography (CH_2Cl_2/CH_3OH 20:1) to afford a yellow oil. Yield: 0.96 g (72%). R_f = 0.32 (CH_2Cl_2/CH_3OH 20:1). ^1H NMR (400 MHz, $CDCl_3$): δ 1.24−1.42 (m, 22H), 1.65−1.67 (m, 2H), 1.82−1.89 (m, 2H), 2.38−2.42 (dd, J = 15.41, 7.58 Hz, 2H), 2.66−2.83 (m, 2H), 2.97−3.05 (m, 2H), 3.41 (t, J = 6.82, 2H), 3.47−3.72 (m, 16H), 3.82−3.99 (m, 4H), 4.22−4.40 (m, 4H). ^{13}C NMR (100 MHz, $CDCl_3$): δ 25.5 (CH_2), 28.5 (CH_2), 29.1 (CH_2), 29.8 (CH_2), 29.8 (CH_2), 29.9 (CH_2), 30.0 (CH_2), 33.1 (CH_2), 33.2 (CH_2), 34.5 (CH_2), 45.8 (CH_2), 48.7 (CH_2), 49.6 (CH_2), 50.3 (CH_2), 50.8 (CH_2), 50.8 (CH_2), 67.3 (CH_2), 67.8 (CH_2), 70.3 (CH_2),

(15) Benco, J. S.; Nienaber, H. A.; McGimpsey, W. G. *Sens. Actuators, B* **2002**, *B85*, 126−130.
(16) Wanichecheva, N.; Benco, J. S.; Lambert, C. R.; McGimpsey, W. G. *Photochem. Photobiol.* **2006**, *82*, 268−273.
(17) Zhang, S.; Echegoyen, L. *J. Am. Chem. Soc.* **2005**, *127*, 2006−2011.

Scheme 1. Synthesis of Compound 1

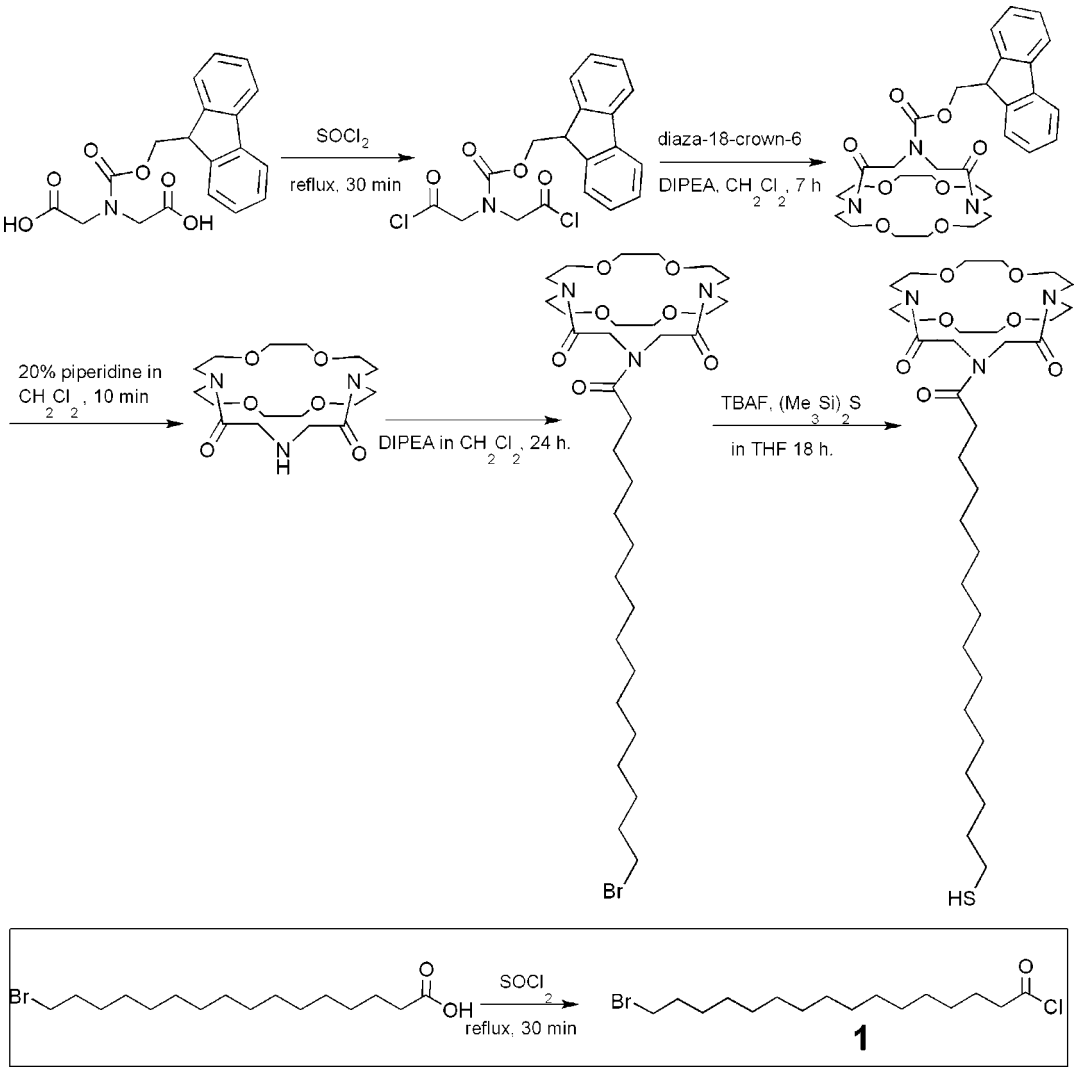

70.9 (CH_2), 71.1 (CH_2), 71.3 (CH_2), 71.8 (CH_2), 72.6 (CH_2), 168.9 (C=O), 169.5 (C=O), 174.5 (C=O).

21-(16-Mercaptohexadecan-1-oyl)-4,7,13,16-tetraoxa-1,10,21-triazabicyclo[8.8.5]tricosane-19,23-dione. Direct mercaptodehalogenation of the alkyl halide was performed according to the procedure reported by Fox et al.[18] In a round-bottom flask, 0.80 g (1.2 mmol) of 21-(16-bromohexadecanoyl)-4,7,13,16-tetraoxa-1,10,21-triazabicyclo[8.8.5]tricosane-19,23-dione was dissolved in 1 mL of dry THF and cooled to −10 °C for 10 min. Then, 0.29 mL of hexamethyldisilathiane ($(Me_3Si)_2S$, 1.4 mmol) and 1.29 mL of tetrabutylammonium fluoride (TBAF, 1.3 mmol, 1.0 M solution in THF with 5% water) were added. The reaction mixture was allowed to warm to room temperature while being stirred for 3 h. The reaction mixture was diluted with 50 mL of dichloromethane and washed three times with saturated aqueous ammonium chloride. The product was obtained by column chromatography (CH_2Cl_2/methanol 20:1) as a yellow oil. Yield: 0.47 g (63%). R_f = 0.27 (20:1 CH_2Cl_2/CH_3OH). ^{1}H NMR (400 MHz, $CDCl_3$): δ 1.24−1.43 (m, 22H), 1.60−1.66 (m, 4H), 2.37−2.41 (dd, J = 15.41, 7.58 Hz, 2H), 2.51 (q, J = 7.58 Hz, 2H), 2.67−2.87 (m, 2H), 2.99−3.06 (m, 2H), 3.50−3.73 (m, 16H), 3.78−3.96 (m, 4H), 4.22−4.38 (m, 4H). ^{13}C NMR (100 MHz, $CDCl_3$): δ 24.9 (CH_2−SH), 25.4 (CH_2), 28.4 (CH_2), 28.7 (CH_2), 29.1 (CH_2), 29.4 (CH_2), 29.7 (CH_2), 29.8 (CH_2), 29.8 (CH_2), 29.9 (CH_2), 29.9 (CH_2), 33.0 (CH_2), 33.1 (CH_2), 34.4 (CH_2), 34.5 (CH_2), 45.8 (CH_2), 48.6 (CH_2), 49.4 (CH_2), 50.0 (CH_2), 50.6 (CH_2), 50.7 (CH_2), 67.2 (CH_2), 67.7 (CH_2), 70.3 (CH_2), 70.8 (CH_2), 71.1 (CH_2), 71.2 (CH_2), 71.7 (CH_2), 72.5 (CH_2), 168.7 (C=O), 169.4 (C=O), 174.4 (C=O). ESI-MS: m/z $C_{32}H_{59}N_3O_7Na$ $(M + Na)^+$ calcd, 652.9; experimental, 652.5.

Preparation of SAMs. Gold slides were purchased from Evaporated Metal Films (EMF, Ithaca, NY). The slides have dimensions of 25 mm × 75 mm × 1 mm with cut edges. They are fabricated on a float glass substrate, coated with 50 Å of chromium followed by 100 Å of gold. The substrates were cut in different sizes according to experimental needs. The slides were cleaned in piranha solution (70% concentrated sulfuric acid and 30% hydrogen peroxide) for 15 min, rinsed with water and ethanol, and dried with nitrogen prior to use. SAMs of the target molecule were prepared by immersing a clean gold slide into a 1−3 mM solution of the thiol in ethanol for up to 48 h. The SAMs were

(18) Hu, J.; Fox, M. A. *J. Org. Chem.* **1999**, *64*, 4959−4961.

rinsed with ethanol and dried with a stream of nitrogen before use.

Instrumentation for SAM Characterization. *Contact Angle.* Contact angle measurements were obtained with a Rame-Hart model 100-00 Goniometer. Drops of water (1−2 μL) were deposited with a micropipet, and the sessile drop contact angle was measured. The average of at least three measurements from three different samples was obtained.

Ellipsometry. Thickness measurements were determined with a manual photoelectric Rudolf 439L633P ellipsometer (Rudolph Instruments; Fairfield, NJ). The change in polarization state of light reflected from the surface was measured at 70° angle of incidence using a HeNe laser (632.8 nm) as the source. The thickness of the film was calculated using the manufacturer's software, assuming values for the extinction coefficient and refractive index of the samples to be 0 and 1.47, respectively. The values reported were the average from three different samples.

Grazing Angle FT-IR. IR spectra were obtained with a Nexus FT-IR spectrometer equipped with a ThermoNicolet grazing angle accessory and a liquid-nitrogen-cooled MCTA detector. The IR beam was incident at 75° on the gold substrates. The optical path was purged with nitrogen gas before and during data acquisition. IR spectra were obtained by collecting 64 scans, with a 4 cm^{-1} resolution, from 4000 to 1000 cm^{-1}. A clean gold substrate was used as a background before the acquisition of each spectrum.

Cyclic Voltammetry. Electrochemical experiments were obtained with an EG&G Princeton Applied Research potentiostat/galvanostat, model 273. A three-electrode setup was used with the SAM as the working electrode (a geometric area of 1 cm^2 was exposed to electrolyte solution), a Ag/AgCl reference electrode, and a Pt wire counter electrode. CVs were measured using a solution containing 1 mM $Ru(NH_3)_6Cl_3$ with 0.1 M tetraethylammonium chloride as the supporting electrolyte.

Impedance Spectroscopy. Impedance measurements were performed using the same three-electrode setup used for cyclic voltammetry. A 1255 HF frequency response analyzer was used in combination with the EG&G Princeton Applied Research potentiostat/galvanostat. Impedance measurements were collected using a background electrolyte solution of 0.1 M tetratethylammonium chloride and titrated with 0.1 M solutions of metal chlorides (MCl, M = Na^+, K^+, Li^+). The electrolyte solution was bubbled with nitrogen at least 5 min before data acquisition. During the measurements, a constant flow of nitrogen was maintained. The impedance plots were obtained in a frequency range of 10 kHz to 0.1 Hz, at an applied dc voltage of −0.5 V vs Ag/AgCl, with an AC amplitude of 5 mV. At least 25 frequencies were used for each measurement, and the impedance data were fitted to an equivalent circuit using the LEVMRUN software package for complex nonlinear least-squares calculations.[19]

Ion-Selective Membrane and Ion-Selective Electrode (ISE) Preparation. A membrane cocktail was prepared to test 21-(16-mercaptohexadecanoyl)-4,7,13,16-tetraoxa-1,10,21triazabicyclo-[8.8.5]tricosane-19,23-dione (**I**) in ISE format. The membrane consisted of 69/30/1 wt % of DOP/PVC/**I**. (DOP = dioctylphthalate) In a flask, 10 mg of **I**, 300 mg of high molecular weight PVC, and 690 mg of DOP were dissolved in 10 mL of THF, and the mixture was sonicated for 10−15 min. The resulting mixture was allowed to cure for 1 day on a glass surface (the thickness of the film after curing was ~200 μm). The film was cut into small round pieces, (diameter = 7 mm) and then incorporated into a Phillips body electrode to which an internal electrolyte (0.1 M KCl) was added.

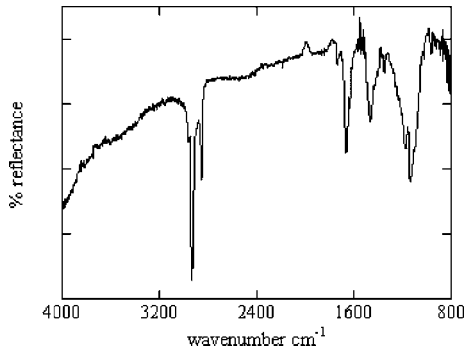

Figure 2. Grazing angle FT-IR spectrum of **I** on gold.

ISE Testing. Potentiometry experiments were obtained with an EG&G Princeton Applied Research model 273 potentiostat/galvanostat. A two-electrode setup was used with the ISE as the working electrode (a membrane area of 0.012 cm^2 was exposed to electrolyte solution) and a Ag/AgCl reference electrode. The ISE response was measured as a function of ion concentration using the relevant chloride salt in 100 mM Tris buffer (pH 7.2). The selectivity of the device was determined as previously described for the SAM electrode and in ref 13.

RESULTS AND DISCUSSION

Monolayer Characterization. Formation of a monolayer on gold was monitored by contact angle, ellipsometry, and FT-IR. The contact angle showed the formation of a slightly hydrophobic layer (48 ± 2°), and ellipsometry demonstrates the formation of a single layer on the surface (layer thickness: 2.2 ± 0.3 nm). The best evidence of deposition of compound **I** on gold comes from the grazing angle FT-IR results (Figure 2), with an absorption peak at 1666 cm^{-1}, corresponding to the carbonyl group of the amide bonds,[20] and a peak at 1130 cm^{-1}, potentially corresponding to the C−H stretch associated with the C−O−C ether bonds. Other significant bands in the IR spectra are the methylene vibrations of the alkyl chain at 2856 and 2927 cm^{-1}.

Sensor Study. The analysis of the SAM-based sensor was carried out following previously reported procedures.[6−9] Cyclic voltammetry in the presence of potassium ferricyanide and potassium chloride showed the formation of a SAM that is insulating to the ferricyanide redox probe. In addition, this experiment shows that the sensor does not bind K^+ to a significant extent. Thus, a positively charged SAM, that is, one with complexed potassium or other ions on the surface, does not block the redox process of a negatively charged species in solution, such as ferricyanide, because of electrostatic attraction between the SAM and the species in solution. The charged SAM acts as an ion gate for the diffusion of electrolyte through the monolayer.[21,22]

(19) Macdonaold, R. *CNLS Immitance, Inversion, and Simulation Fitting Programs for Windows and MS-DOS LEVM Manual 8.0*; University of North Carolina: Chapel Hill, NC, 2003.

(20) Duevel, R. V.; Corn, R. M. *Anal. Chem.* **1992**, *64*, 337−342.

(21) Cheng, Q.; Brajter-Toth, A. *Anal. Chem.* **1992**, *64*, 1998−2000.

(22) Takehara, K.; Ide, Y.; Aihara, M.; Obuchi, E. *Bioelectrochem. Bioenerg.* **1992**, *29*, 103−111.

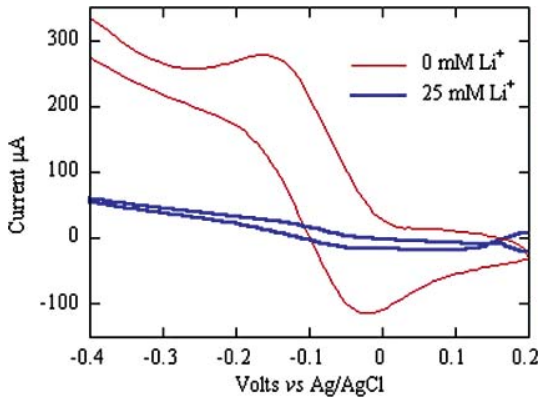

Figure 3. CV in the presence of $Ru(NH_3)_6Cl_3$ showing the ion gate closing effect upon complexation of Li^+ by the sensor. Plot has been smoothed to remove switching transients.

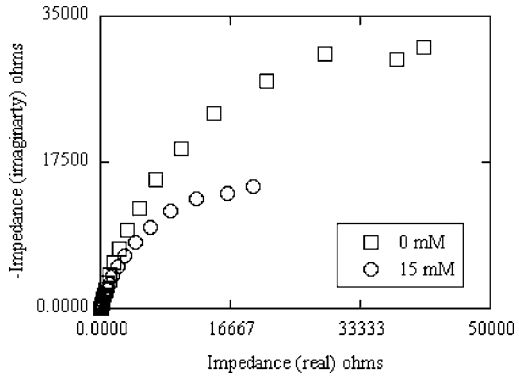

Figure 4. Nyquist plots obtained at −0.5 V vs Ag/AgCl with a supporting electrolyte solution of (1) 0 mM LiCl and 0.1 M tetrabutylammonium bromide and (2) 15 mM LiCl and 0.085 M tetrabutylammonium bromide.

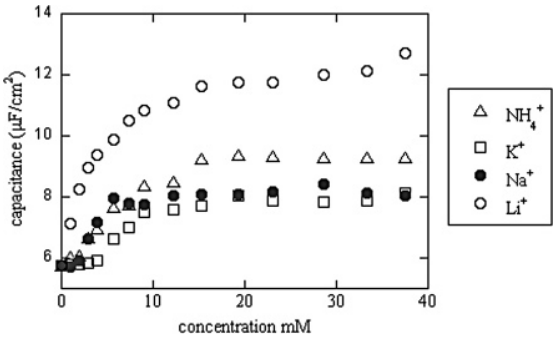

Figure 5. Capacitance as a function of ion concentration for different ions. The results show moderate selectivity for Li^+ detection compared to other ions.

Cyclic voltammetry was used to determine the selectivity of the sensor using another redox probe, hexaammine ruthenium (III) chloride. This was selected on the basis of previous CV studies of sensors that demonstrate that SAMs do not block the redox process of Ru(III), but a SAM with a layer of positive ions complexed with the sensor moiety of the monolayer effectively blocks the redox process of Ru(III).[5−8] The presence of positively charged ions on the surface leads to blocking of the redox process because of electrostatic repulsion between the positively charged SAM and the positively charged ruthenium species.

Figure 3 shows the CV results obtained with hexaammine ruthenium (III) chloride. The experiments were initially carried out with an aqueous solution of 1 mM $Ru(NH_3)_6Cl_3$ and 0.1 M tetrabutylammonium bromide. The film does not block the redox process with this solution. Titration experiments were subsequently conducted by adding aliquots of a solution containing 1 mM $Ru(NH_3)_6Cl_3$ and 0.1 M of a metal chloride or bromide. This ensures that the experiments are carried out with a constant concentration of the redox species and a total 0.1 M concentration of supporting electrolyte, thus eliminating ionic strength effects. The CVs did not change with the addition of potassium, sodium, or ammonium salts. Figure 3 shows the CV after addition of 25 mM LiCl. At this or higher concentration values, the monolayer becomes insulating to the redox process of $Ru(NH_3)_6Cl_3$. Several experiments were carried out to obtain more quantitative results that would give a plot of redox current peak as a function of ion concentration; however, the insulating/conducting effect in the presence of Li^+ ions did not occur as a gradual decrease in conductivity but, rather, as a one-step change in conductivity at a specific concentration value (25 mM), probably the concentration value at which saturation of Li^+ ions on the SAM occurs. This phenomenon may also be related to diffusion of electrolyte through defects on the SAM. A more quantitative analysis was done using impedance techniques to show the ability of the SAM to bind Li^+ ions selectively.

Impedance Results. Experiments in the presence of a background electrolyte solution of 0.1 M tetraethylammonium chloride at −0.5 V vs Ag/AgCl and different concentrations of Li^+, K^+, or Na^+ were obtained. At the applied potential, the experimental Nyquist plots can be modeled using a Randles circuit. The circuit consists of a capacitance in parallel with the monolayer resistance and the Warburg impedance and the solution resistance in series with these components. The Warburg impedance accounts for diffusion processes at low frequencies. The effect of ion complexation should result in changes in the monolayer capacitance, similar to changes in capacitance observed for multilayered films containing metal ions previously discussed. Figure 4 illustrates Nyquist plots obtained at two different concentrations of Li^+ ions. From these Nyquist plots, it was possible to obtain capacitance values for the monolayer that are related to ion concentration in solution. Figure 5 shows a plot of capacitance changes vs ion concentration. The results show that the SAMs have a lower affinity for Na^+ and NH_4^+. NH_4^+ complexation was studied to provide evidence that the supporting electrolyte (tetrabutylammonium bromide or tetraethylammonium chloride) does not significantly interfere in the impedance measurements. Figure 5 demonstrates that SAMs of this sensor molecule have moderate selectivity for Li ions over potassium and sodium ions, with $\log K_{Li^+,Na^+} \sim -1.30$ and $\log K_{Li^+,K^+} \sim -0.92$. Selectivity was calculated by a method used in ion-selective electrode applications.[13,23] Selectivity is represented as a logarithmic value and is calculated using eq 1.

$$\log K_{i,j} = \log([i]/[j]) \qquad (1)$$

Here, [j] is the concentration of the interfering ion in the plateau region of the plot, where the concentration of the interfering ion

(23) Bakker, E.; Buehlmann, P.; Pretsch, E. *Chem. Rev.* **1997**, *97*, 3083−3132.

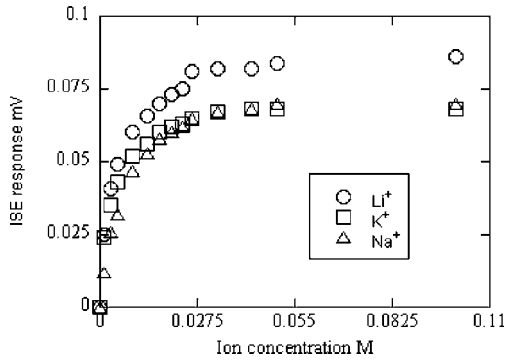

Figure 6. The potential as a function of ion concentration for different ions. The results show moderate selectivity for Li^+ detection compared to other ions.

provides the maximum capacitance response. The concentration of the primary ion, [i], is the concentration that gives the same response as the maximum capacitance produced by the interfering ion, representing a minimum unambiguous detection limit for the primary ion.

Ion-Selective Electrode Results. Compound **I** was also tested in an ISE format. Figure 6 shows the dependence of the potential of **I** on concentrations for lithium, sodium, and potassium. These results illustrate the moderate selectivity of **I** to lithium in comparison with interfering ions, which is consistent with the impedance spectroscopy measurement of the capacitance of this sensor on a gold surface. The results show that the potential increases as a function of ion concentration until it reaches a plateau, beyond which it is constant up to the maximum concentration tested (0.1 M). The selectivity was calculated using eq 1, where i is the lithium ion (primary ion) and j is the interfering ion. Using the above concentrations yields selectivity values for lithium versus sodium, $\log K_{Li^+,Na^+} \sim -0.77$, and lithium versus potassium, $\log K_{Li^+,K^+} \sim -0.82$. Interestingly, these values indicate that the sensor is less selective in the ISE format than in the SAM derivatized electrode. The ionophore of compound **I** has also been modified to contain a fluorophore that transduces the binding of ions via enhanced fluorescence emission (Figure 7).[16] In this

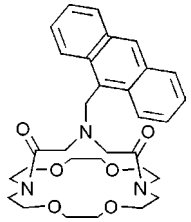

Figure 7. Anthrylmethyl derivative of compound **I**.

modified compound, the ion binding site is essentially the same as in **I**. When measured in solution, selectivity values for **II** were $\log K_{Li^+,Na^+} \sim -3.36$ and $\log K_{Li^+,K^+} \sim -1.77$, showing even higher selectivity. It is interesting to note that the ionophore appears to exhibit the highest selectivity in the most disorganized environment, i.e., solution. This may have implications for the fabrication of a SAM-based ion-selective electrode.

CONCLUSIONS

Monolayers of hexadecanethiol coupled to a bicyclic molecule with the ability to selectively complex Li^+ ions were fabricated. The ability of these monolayers to function as sensors was shown by cyclic voltammetry and impedance spectroscopy techniques. Impedance experiments in the absence of a redox probe (i.e., only supporting electrolyte) provided reproducible data that shows a change in monolayer capacitance upon ion complexation. The compound showed moderate selectivity for complexation of Li^+ ions over other ions, with $\log K_{Li^+,Na^+} \sim -1.30$ and $\log K_{Li^+,K^+} \sim -0.92$. This selectivity is superior to that obtained for **I** in an ISE membrane, $-\log K_{Li^+,Na^+} \sim -0.77$ and $\log K_{Li^+,K^+} \sim -0.82$, although it is somewhat less than that observed in solution for the compound shown in Figure 7 that shows enhanced emission upon ion binding. This study shows that selective ion complexation can be demonstrated on surfaces using an impedance measurement technique.

Received for review February 23, 2006. Accepted May 31, 2006.

AC0603429